

# Quantum Monte Carlo simulations for the Bose-Hubbard model with random chemical potential; localized Bose-Einstein condensation without superfluidity

Mitsuaki Tsukamoto and Makoto Tsubota

*Department of Physics, Osaka City University, Sumiyoshi-Ku, Osaka 558-8585, Japan*

(Dated: November 1, 2018)

The hardcore-Bose-Hubbard model with random chemical potential is investigated using quantum Monte Carlo simulation. We consider two cases of random distribution of the chemical potential: a uniformly random distribution and a correlated distribution. The temperature dependences of the superfluid density, the specific heat, and the correlation functions are calculated. If the distribution of the randomness is correlated, there exists an intermediate state, which can be thought of as a localized condensate state of bosons, between the superfluid state and the normal state.

Bose-Einstein condensation and superfluidity are two important concepts in modern physics. Both of these concepts are characteristic of the ground states of quantum fluids and have been investigated in lots of types of systems. However, the relation between Bose-Einstein condensation and superfluidity remains unclear[1]. Bose-Einstein condensation was first predicted by Einstein for an ideal Bose gas. The Bose-Einstein condensate (BEC) was later observed as the  $\lambda$  transition of strongly-correlated liquid  $^4\text{He}$ , and has recently been realized in dilute atomic gases[2] and excitons in semiconductors[3]. For non-interacting particles, the criterion for Bose-Einstein condensation is that the occupation number for one of the single-particles energy levels should be macroscopic. The general criterion for interacting systems is that the one-particle density matrix  $\rho(\mathbf{x}, \mathbf{y}) = \langle \hat{\psi}^\dagger(\mathbf{x})\hat{\psi}(\mathbf{y}) \rangle$  tends to a constant as  $|\mathbf{x} - \mathbf{y}| \rightarrow \infty$ . In contrast, the term superfluidity originally described a group of experimental phenomena such as frictionless flow and persistent current. After the observation of superfluidity in liquid  $^4\text{He}$ , superfluidity was observed in Fermionic liquid  $^3\text{He}$  and electrons in metals as superconductivity, and is probably realized even in neutron stars. As proposed by Hohenberg and Martin[4], superfluidity is not an equilibrium property of the system, but rather an anomaly of the transport coefficient. However, our understanding of superfluidity is considerably less than our understanding of Bose-Einstein condensation. Our first system showing Bose-Einstein condensation and superfluidity is liquid  $^4\text{He}$ , in which Bose-Einstein condensation and superfluidity occur simultaneously at the  $\lambda$  temperature, but these two concepts are, in principle, not equivalent. Recent studies on disordered Bose systems, such as  $^4\text{He}$  in restricted geometry, describe the separation of BEC and superfluidity. Furthermore, the nature of both Bose-Einstein condensation and superfluidity has been investigated. The present study is an attempt to solve the essential problem in physics by quantum Monte Carlo simulation.

The disordered Bose system is actualized for liquid  $^4\text{He}$  confined in the nano-porous glass[5, 6, 7, 8] and the atomic gas in the optical trap potentials[9]. In particu-

lar, the confinement of  $^4\text{He}$  has been investigated experimentally using various porous glasses, such as Vycor[7], Aerogel[10], and Gelsil[8]. In addition, the confinement of the  $^4\text{He}$  in a uniform-nano-porous medium has also attracted interest[11, 12]. The pressure-temperature phase diagrams change drastically depending on the dimensionalities and pore-sizes of the medium. The superfluidity is suppressed as the pore-size becomes narrow, because the interaction between  $^4\text{He}$  atoms increases with confinement in small pores and applied pressure. For the  $^4\text{He}$  in the FSM[11], which is one-dimensional and uniform porous, there exists a critical pressure above which the normal-fluid state is maintained and the superfluidity does not appear, even at zero temperature, if the diameter of the pore size is less than 2.8 nm.

Recently, low-temperature experiments [8] using  $^4\text{He}$  in nano-porous Gelsil glass, which has a mean pore size of 2.5 nm, revealed that the onset temperature of the superfluidity was lower than the peak temperature of the specific heat that corresponds to the transition temperature to the BEC state. This means that between the SF state and the normal fluid state, an intermediate state, called the localized Bose-Einstein condensate (LBEC) state, exists. In the LBEC state, the  $^4\text{He}$  is in the BEC state, but superfluidity cannot be detected through a torsional oscillator experiment. The LBEC state can be thought of as a localized state of the BECs by the random potential created by the nano-porous medium. Note that for the case of the  $^4\text{He}$  in the uniform medium HMM3[13], which has the same pore size as the mean size of the Gelsil glass, there is no clear indication of the existence of the LBEC state. In addition, the dependences of the superfluidity and the LBEC state on the randomness and pore-size of the porous medium are of particular interest.

The above described experimental results suggest the problem of how the superfluidity depends on the randomness and the finite-size effect of the confinement. In addition,  $^4\text{He}$  in the three-dimensional system of Gelsil glass has different transition temperatures between the BEC and the SF state. This can be realized by cooperation among the randomness and the finite-size effect. This system differs completely from the three-

dimensional bulk  $^4\text{He}$  case, in which the Bose-Einstein condensation and SF transition occur simultaneously at the  $\lambda$  temperature.

In the present paper, we investigate the randomness and its distribution dependence on the Bose system. We consider the Bose-Hubbard model with random chemical potential. Taking a hard-core limit for simplicity, the model Hamiltonian on the three-dimensional cubic lattice with periodic boundary condition is given as

$$\mathcal{H} = -J \sum_{\langle i,j \rangle} (\hat{b}_i^\dagger \hat{b}_j + \text{H.C.}) + \sum_i \mu_i \hat{n}_i, \quad (1)$$

where  $\hat{b}_i^\dagger$  ( $\hat{b}_i$ ) is a boson creation (annihilation) operator,  $\hat{n}_i = \hat{b}_i^\dagger \hat{b}_i$ , and  $\mu_i$  is the random potential that depends on site  $i$ . Here, we define  $\mu_i$  such that it can take two values,  $-\mu_-$  and  $+\mu_+$  ( $\mu_-, \mu_+ > 0$ ). For the random distribution of  $\{\mu_i\}$ , we consider the two cases. One case is a uniformly random distribution, that is, the sites at which  $\mu_i = \mu_+$  ( $-\mu_-$ ) are uniformly distributed with probability  $P_+$  ( $P_- = 1 - P_+$ ). The other case is a correlated distribution, that is, the sites at  $\mu_i = -\mu_-$  tend to make clusters, and the clusters of  $-\mu_-$  are placed randomly such that the density of the sites of  $-\mu_-$  is  $P_-$ . We set the mean size of the clusters to seven to eight sites. We perform quantum Monte Carlo simulation using a directed loop algorithm[14] in order to investigate the Hamiltonian (1) and calculate the temperature dependences of the susceptibility, the SF density, the specific heat, and the two-point correlation function. The random average for the chemical potential is taken over more than 1,024 samples. The dilute Bose system[15] and the mean-field approach[16] have been investigated in terms of the uniformly distributed random potential at finite temperature. The thermodynamic property of the Hamiltonian (1) has not been investigated directly.

Here, we introduce two susceptibilities to determine the transition temperatures corresponding to the two states: the state in which the bosons at  $\mu_i = -\mu_-$  form BEC clusters and the SF state over the entire system. Note that, according to Harris's criterion[17], the universality class of the three-dimensional XY model is not affected by on-site potential. Thus, we can determine the critical temperature from the finite-size scaling (FSS) using the critical exponents of the three-dimensional XY model. We compute the system size dependence of the 'total' susceptibility as follows:

$$\chi_t(L, T) = \frac{1}{\beta N} \sum_{i=1}^N \sum_r \int^\beta \langle b_i^\dagger(0) b_{i+r}(\tau) \rangle d\tau, \quad (2)$$

where  $\tau$  is the imaginary time. We then perform FSS. The critical temperature obtained from the FSS of the  $\chi_t$  corresponds to the onset temperature of the SF density because the correlation length extends over the entire system at the temperature. We call this temperature the

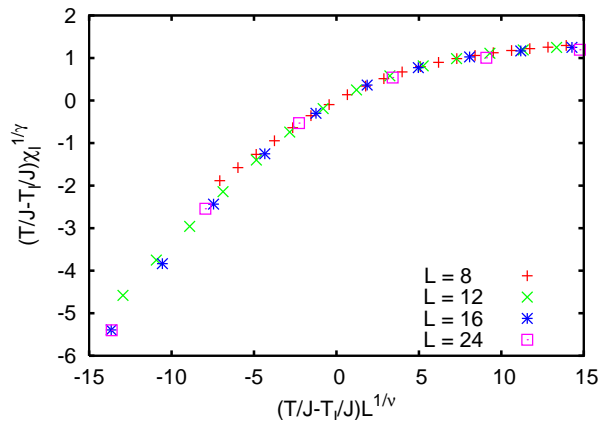


FIG. 1: (color online). Finite-size-scaling plot of the  $\chi_1$  using the critical exponents of the three-dimensional XY model,  $\gamma = 1.3177$  and  $\nu = 0.67155$ . The data of the systems of different sizes follow the same curves, which means that FSS works well. We estimate the transition temperature  $T_1$  to the locally BEC state in this manner. The error bars of the data are smaller than the size of the symbols.

critical temperature  $T_t$ , at which the entire system is in the SF state. Next, we define the local BEC order' and its susceptibility, as follows:

$$\chi_1(L, T) = \frac{1}{\beta N_-} \sum_{i \in \{-\}} \sum_r \int^\beta \langle b_i^\dagger(0) b_{i+r}(\tau) \rangle d\tau, \quad (3)$$

where  $N_-$  is the number of sites at which  $\mu = -\mu_-$  and  $\sum_{i \in \{-\}}$  is a limited summation over these sites. Equation (3) is an integration of the correlation between a site at which  $\mu = -\mu_-$  and a site that is located at a distance  $r$  distant the  $\mu = -\mu_-$  site. From the FSS of the  $\chi_1$ , we define the critical temperature  $T_1$  at which clusters of the  $\mu_i = -\mu_-$  sites are locally in the BEC state.

Figure 1 shows the FSS plot of  $\chi_1$  when  $\mu_- = 2.0$ ,  $\mu_+ = 7.0$ , and  $P_- = 0.2$ , and the random distribution has a correlation. Finite-size scaling using the exponents of the three-dimensional XY model is found to work well for the case in which  $T_1/J = 0.53$ . In contrast, the FSS of the  $\chi_t$  yields the critical temperature  $T_t/J = 0.49$ . For the case in which the random potential is distributed uniformly, there is no difference between  $T_1$  and  $T_t$  within the numerical error. For the case of the correlated random distribution, the bosons at  $\mu_i = -\mu_-$  locally enter the BEC state at  $T_1$  and form clusters, which then link together as the temperature decreases. When the locally correlated clusters percolate through the entire system, superfluidity occurs at  $T_t$ . Since we are interested in the intermediate state between  $T_1$  and  $T_t$ , in the remainder of the present paper, we discuss only the case in which the distribution of the random potential has a correlation.

Figure 2(a) shows the temperature dependence of the SF density [19] for various system sizes, and Fig. 2(b) shows the SF density as a function of the inverse system

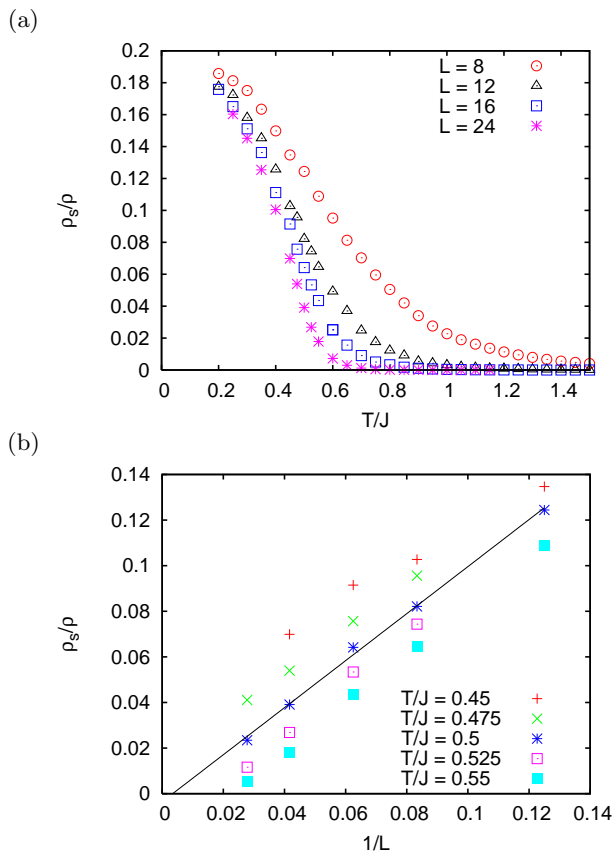


FIG. 2: (a) Temperature dependence and (b) the system size dependence of the SF density for the case in which  $\mu_- = 2.0$ ,  $\mu_+ = 7.0$ , and  $P_- = 0.2$ . The temperatures estimated from FSS for  $\chi_t$  and  $\chi_l$  are  $T_t/J = 0.49$  and  $T_l/J = 0.53$ , respectively. The onset temperature of the superfluidity is consistent with  $T_t$ . The line in (b) is a fitting plot of  $T/J = 0.5$ . (color online).

size  $1/L$ . The line in the Fig. 2(b) is a fitting plot of  $T/J = 0.5$ . The onset temperature of the superfluidity corresponds to the critical temperature  $T_t$ . Hence we find that below  $T_t$  both BEC and superfluidity are achieved over the entire system. We consider the intermediate state of the temperature region between  $T_l$  and  $T_t$  as the state in which the BECs are localized by correlated random chemical potential the entire system does not show the superfluidity.

In Fig. 3, we plot the two-point correlation function

$$G(r) = \frac{1}{N} \sum_i \langle b_i^\dagger b_{i+r} \rangle,$$

as a function of the distance  $r$ . We calculate  $G(r)$  for system sizes of  $L = 16$  and  $20$ . Comparing the results for  $L = 16$  and  $20$ , we find that if  $r < 6$ , there is no difference between the results. Therefore, in order to negate the finite-size effect, we plot only the region of  $r < 6$ . For the ordinary second-order transition belonging to the three-dimensional XY universality class, we

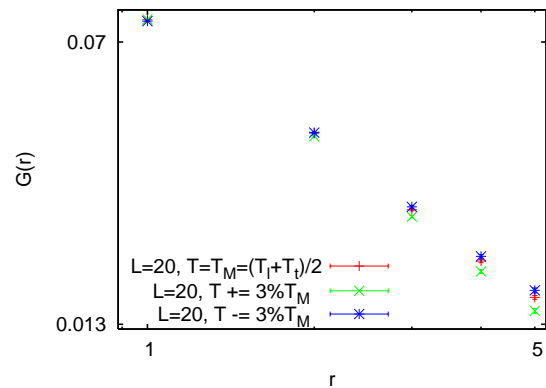


FIG. 3: Two-point correlation function as a function of distance (logarithmic plot). The error bars of the data are smaller than the symbols in the figure. (color online).

have  $G(r) \propto 1/r^{1+\eta} = 1/r^{1.038}$  [18] at the critical temperature, above (below) which the  $G(r)$  decreases exponentially (converges to some constant value) as  $r \rightarrow \infty$ . In the present case, however, the power law behavior is observed for a finite temperature range. Because of the random potential, the critical behavior is unclear, and there appears to be a finite critical region. Since this critical region is small, however, FSS analysis is feasible.

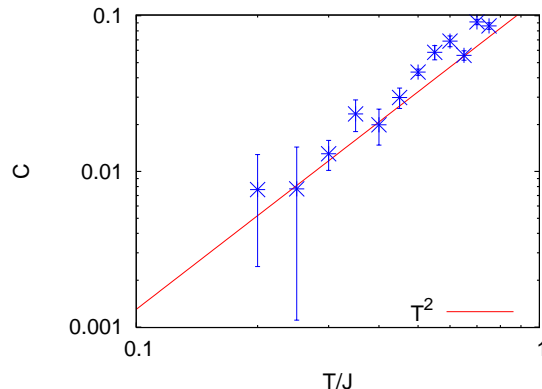


FIG. 4: Logarithmic plot of the temperature dependence of the specific heat. The line in the figure is a fitting plot of  $C \propto T^2$ . (color online).

The temperature dependence of the specific heat is shown in Fig. 4. The line is a curve-fitting plot in which

$$C \sim T^2.$$

The data is well fitted by the line, while for the uniform system  $\mu_i = \mu$ , we find the specific heat behaves as  $C \sim T^3$  at low temperature as a result of the gapless and linear dispersion of the elementary excitations. The  $T$ -square behavior of the specific heat is also observed in the experiment to examine the  $^4\text{He}$  in the Gelsil glass [13]. However, it is thought that  $T$ -square behavior in the experiment is a cross-over of the  $T$ -linear behavior, which

is characteristic of the glass state. Thus, it is expected that  $C \sim T$  as  $T \rightarrow 0$ [13].

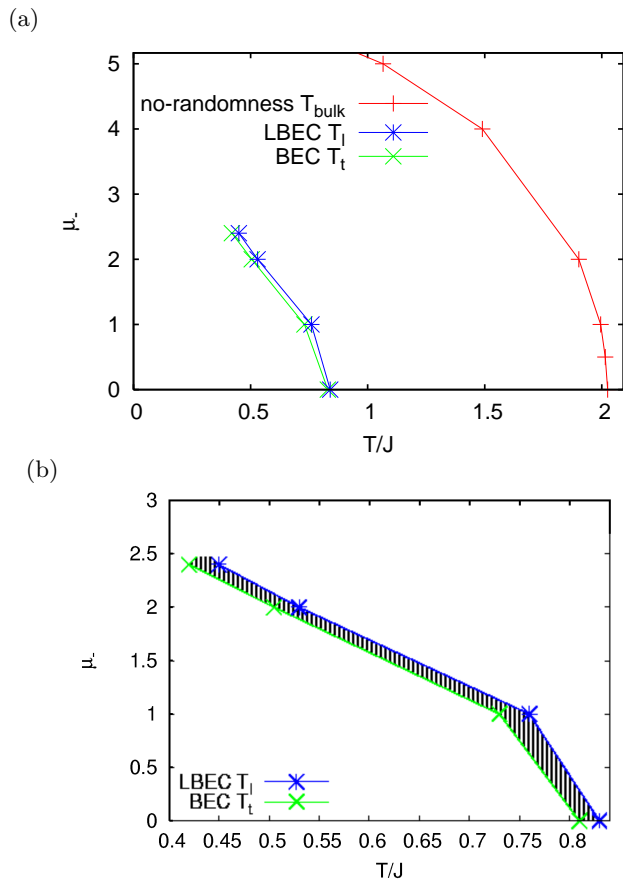


FIG. 5: Phase diagram in the  $\mu_- - T$  plane. (a) An overview of the phase boundaries  $T_{\text{bulk}}$ ,  $T_1$ , and  $T_t$ . The phase boundaries of the system with randomness and non-randomness are approximately parallel. (b) An enlarged view of the LBEC region. The vertical-striped region is the state where the bosons are locally condensed. The error bars of the data are smaller than the size of the symbols. (color online).

Figure 5 shows the phase diagram of the  $\mu_- - T$  plane for  $\mu_+ = 7.0$  and  $P_- = 0.2$ . In the phase diagram, in addition to  $T_t$  and  $T_1$ , we plot the critical temperature  $T_{\text{bulk}}$  of the system with no-randomness. Comparing the system with randomness to that without randomness,  $T_t$  is found to be lower than  $T_{\text{bulk}}$ , which means that the superfluidity is suppressed because of the chemical potential  $\mu_+$ . Comparing  $T_t$  and  $T_1$ ,  $T_t$  is always lower than  $T_1$  at the same  $\mu_-$ . In the vertical-striped region of Fig. 5(b), bosons are locally condensed but the entire system is not in the SF state. Note that the phase boundaries of the system with no-randomness,  $T_t$  and  $T_1$ , are approximately parallel.

In conclusion, we have investigated a Bose-Hubbard model with random chemical potential by quantum Monte Carlo simulation. If the distribution of the random potential has correlation, the localization of the BECs occurs at a temperature above the onset temper-

ature of the superfluidity. We have obtained the phase diagram of the  $\mu_- - T$  plane. In the intermediate state, with respect to the distance, the two-point correlation function displayed power-law behavior.

The reader may wonder whether the locally condensed state obtained in the present study does not correspond exactly to the experimentally observed LBEC state[8]. In the present study, the bosons in the cluster of the  $\mu_i = -\mu_-$  first locally enter the BEC state, and the superfluidity for the entire system then grows as a result of quantum fluctuations as the temperature decreases. On the other hand, the experiment involving the  $^4\text{He}$  in the various nano-porous media, the critical temperature depends on the pore size because of the confinement, where the  $^4\text{He}$  is strongly correlated under the pressure. Each cluster has a different critical temperature depending on the strength of the correlation. As a result, the SF state is experimentally achieved by percolation through the fraction of such LBECs. In the present study, an intermediate state exists between the locally condensed state and the SF state. However, the present situation is not equivalent to that of the experiments, because the correlation of the boson is too strong owing to the hard-core limit.

- 
- [1] *Bose-Einstein Condensation*, edited by A. Griffin, D. W. Snoke, and S. Stringari (Cambridge University Press, Cambridge, 1995).
  - [2] *Bose-Einstein Condensation in Dilute Gases*, C. J. Pethick and H. Smith (Cambridge University Press, Cambridge, 2002).
  - [3] J. P. Eisenstein and A. H. MacDonald, *Nature* **432** 691 (2004)
  - [4] P. C. Hohenberg and P. C. Martin, *Annals of Phys.* **34** 291 (1965).
  - [5] J. D. Reppy, *Physica B* **126**, 335 (1984).
  - [6] J. D. Reppy, *J. Low Temp. Phys.* **87**, 205 (1992).
  - [7] J. R. Beamish *et al.*, *Phys. Rev. Lett.* **50**, 425 (1983).
  - [8] K. Yamamoto *et al.*, *J. Phys. Soc. Jpn.* **77** (2008) 013601, *Phys. Rev. Lett.* **100** (2008) 195301.
  - [9] M. Greiner *et al.*, *Nature* **415**, 39 (2002).
  - [10] M. H. W. Chan *et al.*, *Phys. Rev. Lett.* **61**, 1950 (1988).
  - [11] Y. Matsushita *et al.*, *J. Low Temp. Phys.* **150**, 342 (2008).
  - [12] N. Wada and M. W. Cole, *J. Phys. Soc. Jpn.* **77**, 111012 (2008).
  - [13] K. Shirahama, private communication.
  - [14] O. F. Syljuåsen and A. W. Sandvik, *Phys. Rev. E* **66**, 046701 (2002).
  - [15] M. Kobayashi and M. Tsubota, *Phys. Rev. B* **66**, 174516 (2002).
  - [16] K. V. Krutitsky *et al.*, *New J. Phys.* **8**, 187 (2006).
  - [17] A. B. Harris, *J. Phys. C* **7**, 1671 (1974).
  - [18] M. Campostrini *et al.*, *Phys. Rev. B* **63**, 214503 (2001).
  - [19] The computation of the superfluid density is based on the path-integral method. See E. L. Pollock and D. M. Ceperly, *Phys. Rev. B* **36**, 8343 (1987) .